Antagonism of Central Melanocortin Receptors in Vitro and in Vivo by Agouti-Related Protein

Michael M. Ollmann,* Brent D. Wilson,* Ying-Kui Yang, Julie A. Kerns, Yanru Chen, Ira Gantz, Gregory S. Barsh†

Expression of Agouti protein is normally limited to the skin where it affects pigmentation, but ubiquitous expression causes obesity. An expressed sequence tag was identified that encodes Agouti-related protein, whose RNA is normally expressed in the hypothalamus and whose levels were increased eightfold in *ob/ob* mice. Recombinant Agouti-related protein was a potent, selective antagonist of Mc3r and Mc4r, melanocortin receptor subtypes implicated in weight regulation. Ubiquitous expression of human *AGRP* complementary DNA in transgenic mice caused obesity without altering pigmentation. Thus, Agouti-related protein is a neuropeptide implicated in the normal control of body weight downstream of leptin signaling.

Analysis of mouse obesity mutations has helped define regulatory circuits that govern energy expenditure (*1*). In mice carrying certain alleles of the *Agouti* coat color gene such as *lethal yellow* (A^y) or *viable yellow* (A^{vy}), pleiotropic effects including a yellow coat, obesity, and increased body length are caused by ubiquitous expression of chimeric transcripts encoding a normal Agouti protein (*2–4*). Agouti is a paracrine signaling molecule (*5*) that affects pigmentation by antagonism of the melanocortin 1 receptor (Mc1r) (*6, 7*), one of five related heterotrimeric GTP-binding protein–coupled receptors named for their ability to respond to α-melanocyte stimulating hormone (α-MSH) and adrenocorticotrophic hormone (ACTH) (*8*). Expression and action of Agouti is normally limited to the skin (*3, 5*), but recombinant Agouti protein will also antagonize Mc2r and Mc4r (*6, 9*), expressed primarily in the adrenal gland and the central nervous system (CNS), respectively (*8, 10*).

Using a characteristic pattern of cysteine spacing from the COOH-terminal region of Agouti to search an expressed sequence tag database, we isolated a gene from 129/sv mice and from humans that encodes a protein nearly identical in size and genomic structure to *Agouti* that we named *Agouti-related protein* (*Agrp*) (Fig. 1A). The same gene was recently described by Shutter *et al.* as *Agouti-related transcript* (*11*). Reverse transcriptase–polymerase chain reaction (RT-PCR) and Northern (RNA) hybridization experiments demonstrated that *Agrp* RNA was expressed primarily in the adrenal gland and the hypothalamus (Fig. 1, B and C). To investigate functional overlap between *Agrp* and *Agouti*, we examined whether the steady-state level of *Agrp* RNA would be altered by ectopic expression of Agouti in A^y/a animals. Northern hybridization analysis of hypothalamic and adrenal gland RNA from A^y/a or coisogenic *a/a* animals revealed an ≈fivefold reduction of *Agrp* RNA in the hypothalamus of A^y/a animals (Fig. 1C). We also measured the levels of hypothalamic *Agrp* RNA in *ob/ob* animals and found an ≈eightfold increase relative to coisogenic controls. In the adrenal gland, levels of *Agrp* RNA in A^y/a and nonmutant animals were below the level of detection, but could easily be detected in *ob/ob* animals.

To determine whether AGRP antagonizes melanocortin signaling, we used the baculovirus expression system to produce conditioned media containing recombinant human AGRP, and measured antagonist activity using a *Xenopus* melanophore cell line developed by Lerner and colleagues (*12*). Melanophores provide a rapid and sensitive bioassay for melanocortin agonists and antagonists because pigment granule dispersion induced by α-

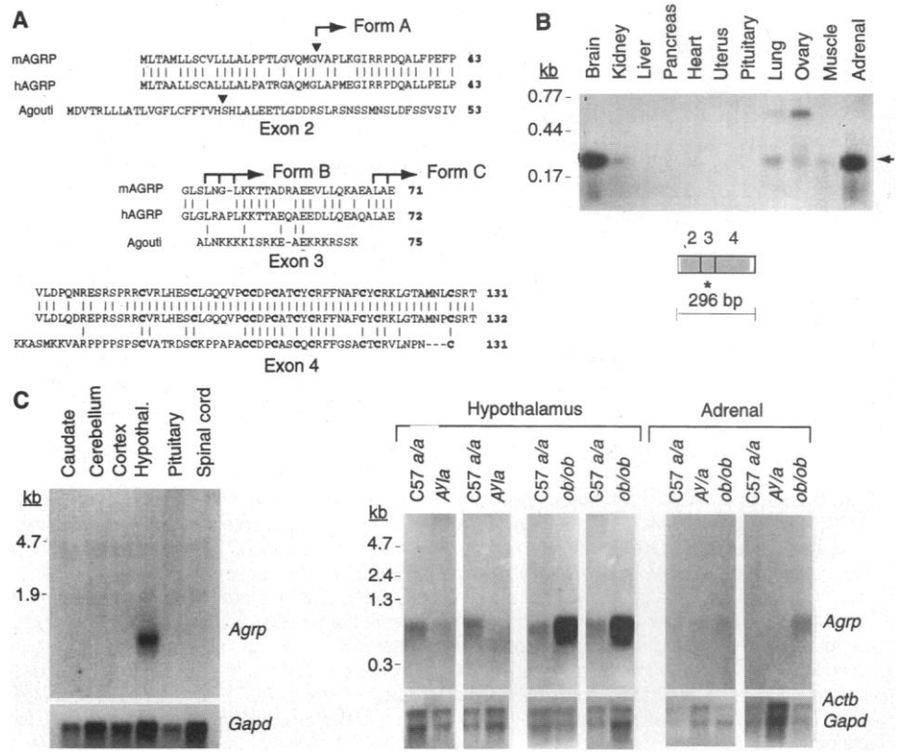

Fig. 1. Structure and expression of *Agrp*. (**A**) Comparison of mouse and human AGRP sequences with that of mouse Agouti. Arrowheads indicate signal sequence cleavage sites; arrows indicate different forms of recombinant AGRP. Abbreviations for the amino acid residues are as follows: A, Ala; C, Cys; D, Asp; E, Glu; F, Phe; G, Gly; H, His; I, Ile; K, Lys; L, Leu; M, Met; N, Asn; P, Pro; Q, Gln; R, Arg; S, Ser; T, Thr; V, Val; W, Trp; and Y, Tyr. Cysteine residues are in bold. (**B**) RT-PCR assay for mouse *Agrp* RNA (*23*). (**C**) Northern hybridization assay for mouse *Agrp* RNA in brain tissues (9 μg, left) or in hypothalamus and adrenal glands of A^y/a and *ob/ob* mice (5 μg, right); each lane represents RNA from a single animal. Relative ratios of *Agrp* RNA determined with a PhosphorImager were based on signal from an exon 4 cDNA probe compared with *Actb* and *Gapd* control probes hybridized to the same blot.

M. M. Ollmann, B. D. Wilson, J. A. Kerns, Y. Chen, G. S. Barsh, Departments of Pediatrics and Genetics and the Howard Hughes Medical Institute, Stanford University School of Medicine, Stanford, CA 94305, USA.
Y.-K. Yang and I. Gantz, Department of Surgery, University of Michigan School of Medicine, Ann Arbor, MI 48109–0682, USA.

*These authors contributed equally to this work.
†To whom correspondence should be addressed at Beckman Center B271A, Stanford University School of Medicine, Stanford, CA 94305–5323, USA. E-mail: gbarsh@cmgm.stanford.edu.

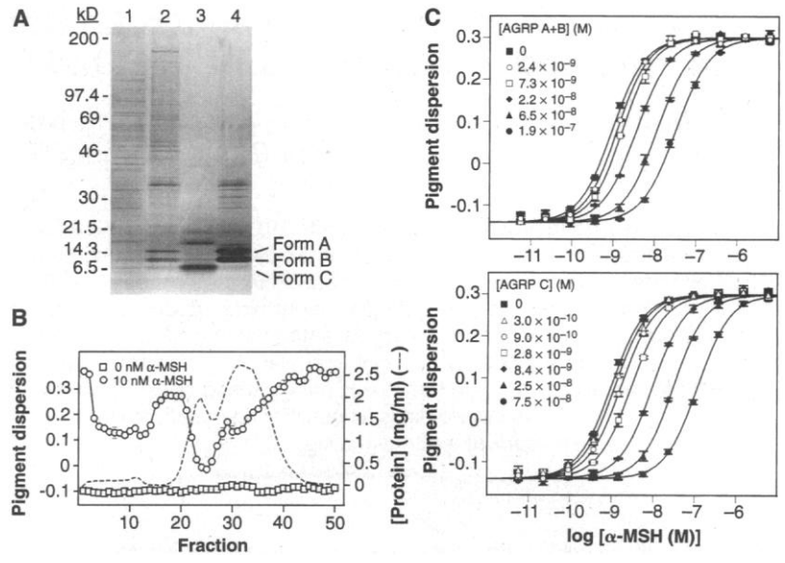

Fig. 2. AGRP activity in *Xenopus* melanophores. (**A**) One microgram of protein from serial steps in the purification procedure analyzed by silver-stained 4 to 20% SDS–polyacrylamide gel electrophoresis. Two liters of conditioned media (lane 1) was applied to a Blue Sepharose Fast Flow Column, then eluted with 40 mM CAPS (pH 10.8), 2.5 M NaCl. Fractions with α-MSH antagonist activity (lane 2) were concentrated (Centriprep 3), buffer-exchanged into 40 mM CAPS (pH 10.8), 20 mM NaCl, applied to a HiTrap Q anion-exchange column, then eluted with a 20 to 800 mM NaCl gradient in 40 mM CAPS (pH 10.8). (**B**) Major peaks of α-MSH antagonist activity in the flow-through (fractions 2 to 13, lane 3) and in fractions 20 to 26 (lane 4) were dialyzed into storage buffer [20 mM Pipes (pH 6.8), 50 mM NaCl]. NH_2-terminal sequencing of the two predominant bands in each peak revealed mature AGRP and two heterogeneous smaller forms as indicated. AGRP purity, estimated by densitometry of a 10-μg sample loaded on a 10% Tricine gel stained with ProBlue, was used to calculate effective concentrations of 40 and 11 μM for form A+B (lane 4) and form C (lane 3), respectively. (**C**) Quantitative α-MSH dose-response analysis of different Agrp forms measured at equilibrium conditions 180 min after addition of AGRP and α-MSH. In the 96-well melanophore assay (*12*), pigment dispersion is calculated as (A_{650} final − A_{650} initial)/A_{650} final, where A_{650} is the absorbance at 650 nm. Data points represent mean ± SEM of triplicate samples.

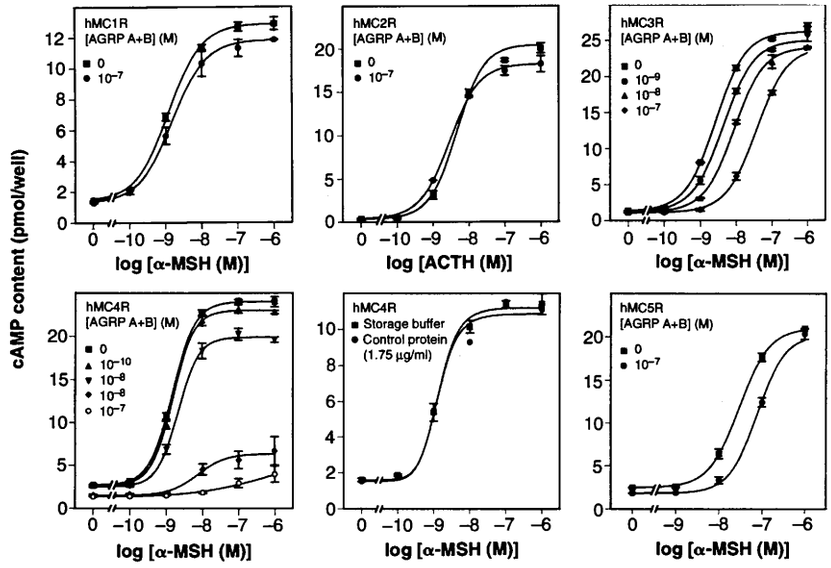

Fig. 3. Effects of AGRP on human melanocortin receptors. 293 cells (hMC1R, hMC3R, hMC4R, or hMC5R) or OS3 cells (hMC2R) stably transfected with the indicated receptor were preincubated with the indicated amounts of AGRP for 30 min; various amounts of α-MSH or ACTH were added for 30 min in the presence of 0.2 mM isobutylmethylxanthine, and total cAMP accumulation was determined on duplicate wells (*9*). Data points represent the mean ± SEM of 2 to 3 independent experiments. As a control for proteins other than AGRP, conditioned media from insect cells infected with an unrelated baculovirus were loaded and eluted from a Blue Sepharose column with conditions identical to those used for AGRP, dialyzed into storage buffer (490 μg/ml), then used at a dilution identical to that used to prepare 100 nM AGRP form A+B. Nanomolar concentrations of AGRP form A+B antagonize the hMC3R and hMC4R but do not meet criteria for competitive antagonism (*15*); therefore, K_B values cannot be calculated.

MSH can be measured in microtiter plates as a change in optical density (*12*). Using the ability of conditioned media to inhibit α-MSH–induced pigment dispersion, we partially purified multiple forms of AGRP that cofractionate with α-MSH antagonist activity by Blue Sepharose and anion-exchange chromatography (Fig. 2). One peak of α-MSH antagonist activity contained mature AGRP with the signal sequence removed (form A) and a mixture of three AGRP fragments cleaved after residues 46, 48, or 50 (form B). The second major peak contained AGRP fragments cleaved after residues 69 or 71 (form C).

Partially purified AGRP forms A+B and form C are potent, specific antagonists of α-MSH–induced pigment dispersion in *Xenopus* melanophores, with calculated antagonist dissociation constant (K_B) values of 7.0 and 1.2 nM, respectively (Fig. 2C). AGRP did not inhibit pigment granule dispersion in the absence of α-MSH and did not inhibit pigment granule dispersion induced by forskolin, a direct activator of adenylate cyclase (*13*).

To examine the selectivity of AGRP for human melanocortin receptors, we added various concentrations of AGRP form A+B to cell lines that had been stably transfected with each of the five different receptor subtypes, then measured the ability of α-MSH or ACTH to induce adenosine 3′,5′-monophosphate (cAMP) accumulation. At concentrations up to 100 nM, AGRP had no effect on hMC1R or hMC2R, and only slightly inhibited hMC5R (Fig. 3). By contrast, AGRP concentrations of 1 nM or more caused a dose-dependent inhibition of α-MSH–induced cAMP accumulation mediated by hMC3R and hMC4R.

Because AGRP form C can antagonize α-MSH in melanophores (Fig. 2) or in Mc4r-transfected cells (*13*), the COOH-terminal cysteine-rich region is probably sufficient for biologic activity, as is the case for Agouti (*14*). Sequence comparison of AGRP and Agouti highlights a short region of similarity beginning with the third Cys residue, CCDPCAXCXCRFF, that may contain determinants required for melanocortin antagonism (Fig. 1A). Nonetheless, the exact biochemical mechanism by which these proteins act is not clear. Most evidence favors competitive antagonism,

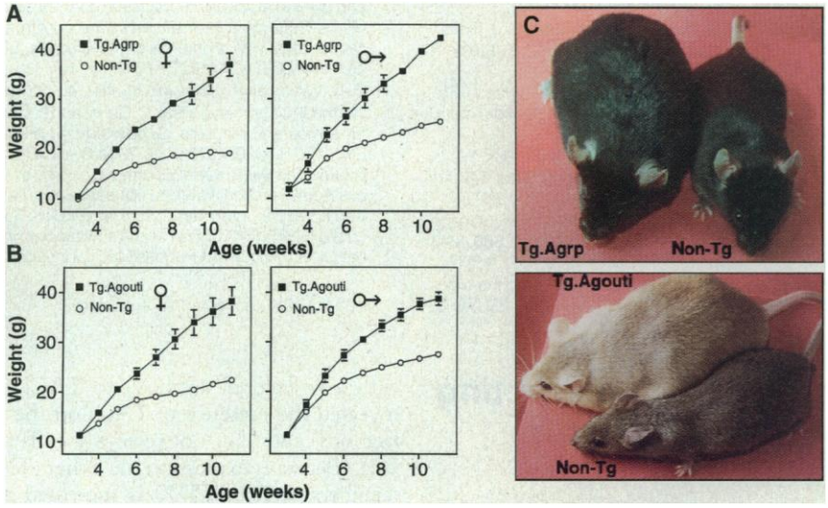

Fig. 4. Effects of AGRP or human Agouti in transgenic mice. A β-actin human *AGRP* cDNA construct nearly identical to one described previously for human Agouti (*24*) was injected into F_2 (C57BL/6J × CBA/J) embryos. One of six F_0 founders (*17*) was bred to C57BL/6J animals. At 11 weeks of age, F_1 transgenic animals (females: $n = 4$; males: $n = 3$) weighed significantly more than nontransgenic littermates (females: $n = 6$, $P = 0.00005$; males: $n = 6$; $P = 0.00002$). The time of onset and level of weight gain caused by the AGRP transgene (**A**) were similar to those caused by the Agouti transgene (**B**), but the AGRP transgene had no effect on pigmentation (**C**). Data points represent the mean ± SEM.

whereby α-MSH and Agouti (or AGRP) bind to mutually exclusive sites on melanocortin receptors (*14*). The effects of AGRP on melanophores are consistent with competitive antagonism, because increasing amounts produced a proportionate and parallel displacement of the α-MSH dose-response curve without affecting maximal signaling (Fig. 2C). For the hMC4R, however, AGRP concentrations of 10 and 100 nM produced a decrease in basal levels of cAMP accumulation, as well as a decrease in the maximal level of α-MSH–induced cAMP accumulation (Fig. 3), neither of which is consistent with competitive antagonism (*15*). It has been proposed that some effects of Agouti are mediated by alterations in calcium flux (*16*), an intriguing finding given the similarity in cysteine spacing between Agouti, AGRP, and certain calcium channel antagonists (*4*). It is possible that Agouti or AGRP does not bind directly to melanocortin receptors or binds to more than one cell surface protein, uncertainties that may be resolved by studies of Agouti and AGRP binding.

To determine whether or not Agouti and AGRP have comparable effects in vivo, we constructed transgenic mice in which the human *AGRP* cDNA was controlled by the ubiquitously expressed β-actin promoter. Weight gain of six independent transgenic founders was significantly increased over nontransgenic littermates (*17*), and a transgenic line was established. Among F_1 animals carrying the β-actin AGRP transgene, increased weight gain was detectable at 4 weeks of age, reached levels 100 or 70% above that of nontransgenic females or males, respectively, and was nearly indistinguishable from that caused by a β-actin Agouti transgene (Fig. 4). Body length and food consumption were also increased by the AGRP transgene (*17*). By contrast, none of 15 animals carrying the AGRP transgene exhibited a difference in coat color from their nontransgenic littermates (Fig. 4). Thus, although AGRP mimics the effect of Agouti on weight gain, body length, and food consumption, it has no effect on pigmentation.

Given the eightfold increase of hypothalamic expression in *ob/ob* mice, we propose that *Agrp* normally regulates body weight via central melanocortin receptors, analogous to the relation between Agouti and the Mc1r for regulation of pigmentation. Huszar *et al.* (*18*) have shown that Mc4r-deficient animals develop obesity and metabolic derangements that mimic those in $A^y/-$ mice, which suggests that obesity caused by ubiquitously expressed *Agrp* or *Agouti* is mediated largely by Mc4r. However, AGRP may also be a physiologic ligand of Mc3r (Fig. 3), which has been implicated in Agouti-induced obesity (*19*) and whose CNS expression (*20*) more closely matches that of *Agrp*. In the brain, *Agrp* RNA is localized primarily to the arcuate nucleus and median eminence (*11*), but unlike Agouti, which has a very small sphere of action in vivo (*3*), AGRP may diffuse more widely, particularly if it is processed to a smaller COOH-terminal form in vivo. AGRP is also produced by the adrenal gland but does not affect hMC2R and therefore may act at a more distant site.

What advantages do endogenous receptor antagonists such as Agouti or AGRP offer for homeostatic regulation? In the case of melanocortins, which activate five receptors to varying extents, an antagonist limited in its tissue distribution or biochemical specificity, or both, allows individual regulation of receptor subtype signaling. Melanocortin receptors were identified on the basis of their response to the agonist α-MSH (*6*), but physiologic signaling via Mc1r is regulated mainly by alterations in levels of the antagonist, Agouti. Similarly, regulation of Mc3r or Mc4r signaling could be mediated primarily by changes in Agrp expression rather than proopiomelanocortin, the precursor of α-MSH and ACTH. Agouti or AGRP, or both, may also transduce a signal via melanocortin receptors independent of melanocortin binding (*21*), consistent with the effects we observed on basal levels of cAMP accumulation.

Leptin deficiency lies upstream of *Agrp* expression, directly or indirectly, but other signaling systems implicated in energy balance (*22*) may also regulate *Agrp* expression. Additional studies based on gene targeting may help to place *Agrp* in a genetic pathway for feeding behavior, which should be useful in understanding and developing treatments for disorders of body weight regulation.

REFERENCES AND NOTES

1. Y. Zhang *et al.*, *Nature* **372**, 425 (1994); L. A. Tartaglia *et al.*, *Cell* **83**, 1263 (1995); K. Noben-Trauth, J. K. Naggert, M. A. North, P. M. Nishina, *Nature* **380**, 534 (1996); J. K. Naggert *et al.*, *Nature Genet.* **10**, 135 (1995).
2. D. M. J. Duhl, H. Vrieling, K. A. Miller, G. L. Wolff, G. S. Barsh, *Nature Genet.* **8**, 59 (1994); E. J. Michaud *et al.*, *Genes Dev.* **8**, 1463 (1994).
3. W. K. Silvers, in *The Coat Colors of Mice* (Springer-Verlag, New York, 1979), pp. 6–44.
4. J. Manne, A. C. Argeson, L. D. Siracusa, *Proc. Natl. Acad. Sci. U.S.A.* **92**, 4721 (1995).
5. S. J. Bultman, E. J. Michaud, R. P. Woychik, *Cell* **71**, 1195 (1992); M. W. Miller *et al.*, *Genes Dev.* **7**, 454 (1993).
6. D. S. Lu *et al.*, *Nature* **371**, 799 (1994).
7. L. S. Robbins *et al.*, *Cell* **72**, 827 (1993).
8. K. G. Mountjoy, L. S. Robbins, M. T. Mortrud, R. D. Cone, *Science* **257**, 1248 (1992).
9. Y. K. Yang *et al.*, *Mol. Endocrinol.* **11**, 274 (1997).
10. I. Gantz *et al.*, *J. Biol. Chem.* **268**, 15174 (1993); K. G. Mountjoy, M. T. Mortrud, M. J. Low, R. B. Simerly, R. D. Cone, *Mol. Endocrinol.* **8**, 1298 (1994).
11. J. R. Shutter *et al.*, *Genes Dev.* **11**, 593 (1997).
12. J. M. Quillan, C. K. Jayawickreme, M. R. Lerner, *Proc. Natl. Acad. Sci. U.S.A.* **92**, 2894 (1995); N. Potenza and M. R. Lerner, *Pigment Cell Res.* **5**, 372 (1992).
13. M. M. Ollmann, Y.-K. Yang, B. D. Wilson, I. Gantz, G. S. Barsh, unpublished observations.
14. D. H. Willard *et al.*, *Biochemistry* **34**, 12341 (1995); S. G. Blanchard *et al.*, *ibid.*, p. 10406.
15. T. P. Kenakin, *Can. J. Physiol. Pharmacol.* **60**, 249 (1982).
16. M. B. Zemel *et al.*, *Proc. Natl. Acad. Sci. U.S.A.* **92**, 4733 (1995); J. H. Kim *et al.*, *FASEB J.* **10**, 1646 (1996).

17. Individually caged mice had free access to standard Chow and were treated in accordance with Stanford guidelines. At 11 weeks of age, female F_0 animals weighed 30.5, 35.5, and 41.9 g, and male F_0 animals weighed 32.4, 34.8, and 43 g—significantly more than nontransgenic littermates (females: 21.1 ± 2.0 g, $n = 10$, $P = 0.02$; males: 26 ± 2.0 g, $n = 5$, $P = 0.03$, student's t test). At 15 weeks of age, body length of F_1 transgenic animals (10.5 ± 0.1 cm, $n = 4$) was more than that of nontransgenic littermates (9.18 ± 0.2 cm, $n = 10$, $P = 0.0002$). Food consumption measured over a 7-day period at 12 weeks of age for F_1 transgenic animals (27.9 ± 5.4 g, $n = 4$) was more than that of nontransgenic littermates (21.9 ± 2.8 g, $n = 5$, $P = 0.03$).
18. D. Huszar *et al.*, *Cell* **88**, 131 (1997).
19. W. Fan, B. A. Boston, R. A. Kesterson, V. J. Hruby, R. D. Cone, *Nature* **385**, 165 (1997); L. L. Kiefer *et al.*, *Biochemistry* **36**, 2084 (1997).
20. L. Roselli-Rehfuss *et al.*, *Proc. Natl. Acad. Sci. U.S.A.* **90**, 8856 (1993); I. Gantz *et al.*, *J. Biol. Chem.* **268**, 8246 (1993).
21. W. Siegrist *et al.*, *J. Recept. Signal Transd. Res.* **17**, 75 (1997); G. Hunt and A. J. Thody, *J. Endocrinol.* **147**, R1 (1995); C. Sakai *et al.*, *EMBO J.* **16**, 3544 (1997).
22. J. C. Erickson, G. Hollopeter, R. D. Palmiter, *Science* **274**, 1704 (1996); D. Qu *et al.*, *Nature* **380**, 243 (1996); M. Spina *et al.*, *Science* **273**, 1561 (1996).
23. RNA (1 μg) was amplified by RT-PCR with the oligonucleotides 5′-ATGCTGACTGCAATGTTGCTG-3′ and 5′-GGTACCTGCTGTCCCAAGCAG-3′; identity of the 296–base pair product was confirmed by hybridization with an internal oligonucleotide, 5′-CTGCAGAAGGCAGAAGCTTTG-3′.
24. B. D. Wilson *et al.*, *Hum. Mol. Genet.* **4**, 223 (1995).
25. We thank M. Lerner, J. Rine, T. Gunn, and F. Chehab for advice and reagents. Supported by NIH grants EY07106 and GM07365 to M.M.O., J.A.K., and B.D.W. This work was supported in part by a Veterans Administration Award to I.G. and by grants from the NIH to the University of Michigan (P30DK-34933) and to G.S.B. (DK28506), who is an Associate Investigator of the Howard Hughes Medical Institute.

16 May 1997; accepted 19 August 1997

NF-AT Activation Induced by a CAML-Interacting Member of the Tumor Necrosis Factor Receptor Superfamily

Götz-Ulrich von Bülow and Richard J. Bram*

Activation of the nuclear factor of activated T cells transcription factor (NF-AT) is a key event underlying lymphocyte action. The CAML (calcium-modulator and cyclophilin ligand) protein is a coinducer of NF-AT activation when overexpressed in Jurkat T cells. A member of the tumor necrosis factor receptor superfamily was isolated by virtue of its affinity for CAML. Cross-linking of this lymphocyte-specific protein, designated TACI (transmembrane activator and CAML-interactor), on the surface of transfected Jurkat cells with TACI-specific antibodies led to activation of the transcription factors NF-AT, AP-1, and NFκB. TACI-induced activation of NF-AT was specifically blocked by a dominant-negative CAML mutant, thus implicating CAML as a signaling intermediate.

We identified proteins that can interact with CAML in a two-hybrid screen (*1*, *2*). To determine if any of these CAML-binding proteins affected signaling in T cells, we examined their ability to modulate activity of the Ca^{2+}-dependent transcription factor NF-AT (*3*). Overexpression of the two-hybrid clones in Jurkat T cells revealed that expression of one clone (encoding the TACI protein) led to activation of NF-AT, suggesting that TACI may lie in the same signaling pathway as CAML. The deduced amino acid sequence of TACI (Fig. 1A) (*4*) includes a single hydrophobic region (residues 166 to 186) that has features of a membrane-spanning segment. Analysis of the protein sequence (*5*) predicted extracellular exposure for the NH_2-terminus with a cytoplasmic COOH-terminus. Although TACI lacks an NH_2-terminal signal sequence, the presence of an upstream stop codon indicates that the complete open reading frame is contained within the clone (*6*). The predicted cell-surface location of TACI was confirmed in intact Cos-7 cells transfected with an expression plasmid encoding TACI with an NH_2-terminal FLAG epitope tag. Staining with monoclonal antibody to FLAG revealed TACI localized to the cell surface (Fig. 2A). TACI is therefore a type III transmembrane protein with an extracellular NH_2-terminus in the absence of a cleaved signal sequence (*7*). Inspection of the TACI protein sequence also revealed two repeated regions (residues 33 to 66 and 70 to 104) that are 50% identical. A PROSITE motif search (*8*) identified this repeated region as a cysteine-rich motif characteristic of the tumor necrosis factor receptor (TNFR) superfamily. Comparison of TACI with other members of TNFR superfamily (Fig. 1B) demonstrates the similarity between these domains, with the best match to cysteine-rich domains of DR3 (also known as Wsl-1, Apo-3, or TRAMP) (*9*).

Northern blot analysis of TACI mRNA demonstrated a 1.4-kb transcript expressed in spleen, small intestine, thymus, and peripheral blood lymphocytes, suggesting that a single TACI transcript is present in both T and B lymphocytes (Fig. 2B). Specific antibody staining of peripheral blood cells with a polyclonal antibody to TACI (*10*) revealed the presence of TACI on the surface of B cells, but not resting T cells (Fig. 2C). Because expression of other TNFR members such as CD30 is increased after activation of T lymphocytes (*11*) and because TACI appears to be expressed in thymocytes, we examined T cells activated with ionomycin and phorbol ester. Such treatment of T cells induced the synthesis of cell-surface TACI in 54% of CD2-positive cells within 48 hours (Fig. 2D). This subset was equally distributed between CD4 and CD8 cells. Stimulation of interleukin-2 (IL-2)–dependent T cells with antibodies to CD3 and CD28 also induced expression of TACI. A reverse transcriptase–polymerase chain reaction assay revealed TACI message in resting B cells but not in T cells, unless they were activated (*6*).

Neither TACI mRNA nor protein could be detected in untransfected Jurkat cells expressing the SV40 large T-antigen (TAg), either unstimulated or treated with phorbol myristyl acetate (PMA) and ionomycin (*6*). To assess the effect of TACI on NF-AT activity in T cells, we transiently expressed the protein in TAg Jurkat cells along with a secreted alkaline phosphatase reporter driven by the NF-AT–binding sequences from the IL-2 promoter (*12*, *13*, *14*). TACI overexpression could partially replace the requirement for PMA and ionomycin in this assay for maximal activation of the NF-AT reporter. The addition of antibodies to TACI to the cells increased NF-AT activation up to sevenfold (Fig. 3A), demonstrating that TACI responds to cross-linking at the cell surface. This affinity-purified antibody to TACI had no effect on control transfected cells. To further verify the specificity of the response, we transfected cells with an NH_2-terminal FLAG-epitope–tagged TACI expression plasmid and incubated them with the M2-FLAG monoclonal antibody (*15*). This treatment gave a similar increase in NF-AT activity (Fig. 3A). The degree of NF-AT activation varied among different experiments because of transfection efficiency, but was typically 40 to 100% of the maximal re-

G.-U. von Bülow, Department of Experimental Oncology, St. Jude Children's Research Hospital, 332 North Lauderdale, Memphis, TN 38105, USA.
R. J. Bram, Departments of Experimental Oncology and Hematology/Oncology, St. Jude Children's Research Hospital, 332 North Lauderdale, and Department of Pediatrics, University of Tennessee, Memphis, TN 38105, USA.

*To whom correspondence should be addressed. E-mail: richard.bram@stjude.org